Quantitative MR imaging method

Bruno Madore[1], Cheng-Chieh Cheng[2], and Chang-Sheng Mei[1]

[1]*Department of Radiology, Harvard Medical School, Brigham and Womens' Hospital, Boston, MA, United States,* [2]*Department of Electrical Engineering, National Taiwan University, Taipei, Taiwan*

Target Audience: Researchers and clinicians interested in quantitative MR imaging.

Purpose: A patient receiving a typical MR exam can expect to lie in the scanner for as long as 45 min or so as the anatomy of interest gets repeatedly imaged, using a variety of tissue contrasts. The proposed approach allows the main MR parameters such as M_0, T_1, R_2, R_2', B_1 and B_0 to be rapidly and quantitatively evaluated, so that any desired image contrast could, in principle at least, be computed rather than acquired.

$$|S_{i,k}(t)| \propto e^{-(R_2+R_2')\times t}, k \geq 0; \; |S_{i,k}(t)| \propto e^{-(R_2-R_2')\times t}, \quad k<0 \quad [1]$$

$$\ln(|S_{i,k}(TE_{i,j,k})|) = \begin{cases} \ln(|S_{i,k}(0)|) - TE_{i,j,k} \times (R_2 + R_2'), & k \geq 0 \\ \ln(|S_{i,k}(0)|) - TE_{i,j,k} \times (R_2 - R_2'), & k < 0 \end{cases} \quad [2]$$

$$X_{i,k} = 1 - 2 \times (F_{i,k}^- - F_{i,k}^+) \Big/ \left(F_{i,k}^- + \overline{F_{i,-k}^-}\right), \quad |k|>0 \quad [3]$$

$$(X_{1,k}c_1 - 1)^{\frac{TR_2}{TR_1}} \times (X_{2,k} - c_2) - (X_{2,k}c_2 - 1) \times (X_{1,k} - c_1)^{\frac{TR_2}{TR_1}} = 0, \quad |k|>0 \quad [4]$$

$$T_{1,i,k} = TR_i \Big/ \ln\left(\frac{X_{i,k} \times c_i - 1}{X_{i,k} - c_i}\right), \quad |k|>0 \quad [5]$$

$$M_{0,i,k} = \left((F_{i,0}^+ - c_i \times F_{i,0}^-) + (F_{i,0}^- - c_i \times F_{i,0}^+) \times e^{-\frac{TR_i}{T_1}} \right) \Big/ s_i \times \left(1 - e^{-\frac{TR_i}{T_1}}\right) \quad [6]$$

$$F_{i,k}^{+,-} = +|F_{i,k}^{+,-}|, \quad k \geq 0; \quad F_{i,k}^{+,-} = -|F_{i,k}^{+,-}|, \quad k<0 \quad [7]$$

Methods: Quantitative MR imaging performed within a practical scan time has been a quest for the MR community for a long time, with inspired contributions such as GESFIDE[1], DESPOT[2], MP-DESS[3], TESS[4] and MR fingerprinting[5]. The method proposed here allows all of the main MR parameters to be calculated from data acquired from a single sequence. Previous methods may have targeted subsets of parameters for quantitative evaluation and/or required different sequences for different parameters. MR fingerprinting is a practical approach that also aims at evaluating all main parameters, but uses comparisons and matching with a databank of simulated results to do so. Because parameters are directly calculated here instead, a leaner approach that acquires only the minimum amount of data can be more naturally obtained.

The pulse sequence employed is a triple-pathway steady-state sequence similar to that used in TESS[4] (Fig. 1). Two scans, either sequential are interleaved, are performed with different nominal flip angles, $\hat{\alpha}_1$ and $\hat{\alpha}_2$, and/or different TR settings, TR_1 and TR_2. $TE_{i,j,k}$ represents the echo time associated with the j^{th} echo for the k^{th} pathway, as sampled during the i^{th} scan. During TR the signal $S_{i,k}(t)$ varies as described in Eq. 1[6], where $T_2 = 1/R_2$ and $T_2^* = 1/(R_2+R_2')$, leading to the linear system in Eq. 2.

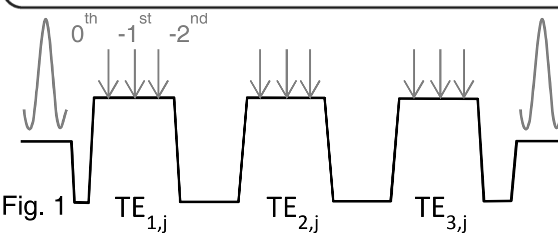

Fig. 1

Using R_2 and R_2' as found from Eq. 2, signals at t=0 and t=TR can be calculated. The notation F_k and Z_k represents transverse and longitudinal magnetization states[7] and superscripts -, + and ⇒ are used to distinguish between the moments just before, just after and a time TR after an RF pulse. In a sequential acquisition, $Z_{i,k}^{\Rightarrow} = Z_{i,k}^-$, while in an interleaved acquisition $Z_{i,k}^{\Rightarrow} = Z_{h(i),k}^-$ where the $h(i)$ function returns the scan number that differs from i in a two-scan acquisition, i.e., $h(1) = 2$ and $h(2) = 1$. In the interest of space, only the sequential case is presented below. An important parameter referred to as 'mixing factor', $X_{i,k}$, is defined in Eq. 3. The flip angle α_1, proportional to the B_1 field, is found by solving Eq. 4, where $c_i = \cos(\alpha_i)$. To make Eq. 4 a single-unknown equation of α_1, the relationship between c_2 and α_1 must be known. In the small-flip angle and/or hard-pulse regime, $c_2=\cos(\alpha_1 \times \hat{\alpha}_2 / \hat{\alpha}_1)$, while in the case of large slab-selective pulses simulations are used to evaluate g(·) as in $c_2 = g(\alpha_1, \hat{\alpha}_1, \hat{\alpha}_2)$.

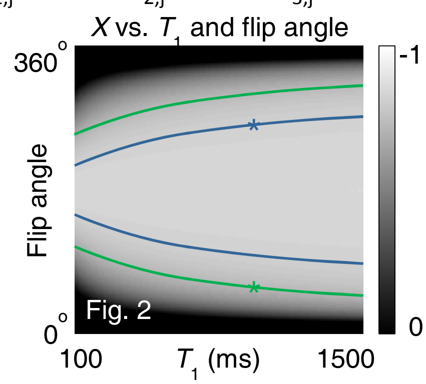

Fig. 2

Once α_1 is found, T_1 and M_0 can be readily obtained from Eqs 5-6, where $s_i = \sin(\alpha_i)$. The presence of indices for T_1 and M_0 in Eqs 5-6 reflects the fact they can be obtained in independent ways, which are averaged to get a final value. In cases where more than one root can be found for Eq. 4, common sense points to the correct one: M_0 and T_1 are positive, $\alpha_1 \approx \hat{\alpha}_1$ near the center of the slab, and the B_1 field should be reasonably smooth.

The F and Z magnetization states are complex numbers, but great simplification can be derived from the realization that imperfections in the B_0 and/or B_1 fields tend to affect the phase of the measured F values but not their magnitude. By using real values for F as shown in Eq. 7, Eqs 3-6 can be solved using real rather than complex numbers. Phase information can be used, independently, to obtain a measure of the frequency offset.

Results: Simulating the effect of RF pulses and gradients on a virtual object led to simulated MR signals that were processed using the equations above. In the absence of noise, all parameters could be evaluated with essentially perfect accuracy: M_0, T_1, R_2, R_2', flip angle and frequency offset. The key parameter $X_{i,k}$ is plotted in Fig. 2 for a range of α and T_1 values to provide a visual representation of how the method works (T_2=70 ms and TR=50 ms were used). A single scan would not suffice to pinpoint both α and T_1 for a given value of X (e.g., blue lines). But two scans along with a known relation between them, for example $\alpha_2 = 2\times\alpha_1$, can allow a solution to be found ('*' marks in Fig. 2).

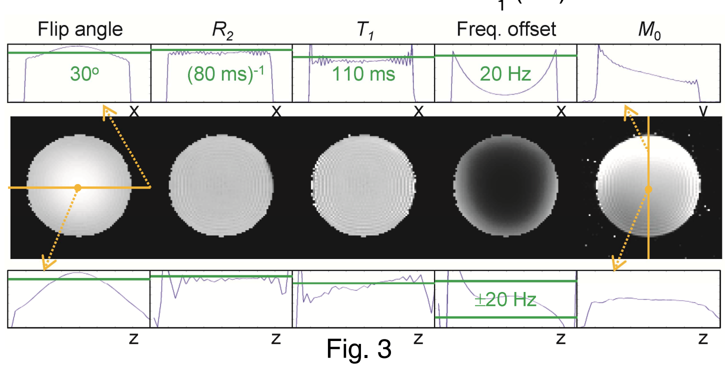

Fig. 3

Phantom data have been acquired and processed as described above and results are shown in Fig. 4 (TR = 30 ms, 4 echoes per TR per pathway, $\hat{\alpha}_2 / \hat{\alpha}_1$ = 10, matrix size = 80×80×40, 192 s for 3D acquisition, selective Gaussian-shaped RF excitations). Nominal and independently measured values are shown in green. While some systematic errors could be readily noticed (e.g., ringing, linear trend for T_1 along z) very little noise could be seen in the results even though no filtering was applied.

Discussion and conclusion: The proposed approach allows M_0, T_1, R_2, R_2', B_1 and B_0 to be evaluated with relatively short scan time over a 3D volume. At the time of writing, optimizations of acquisition parameters had not yet been performed. But as can be seen from the different curvature of lines above and below the 180° value in Fig. 2, considerable improvements in stability appear to be gained when working with greatly different $\hat{\alpha}_1$ and $\hat{\alpha}_2$ settings.

References: [1] Ma J, Wehrli FW. J Mag Res B 1996, 111:61–9. [2] Deoni SCL, Rutt BK, Peters TM. MRM 2003, 49:515–26.
[3] Stöcker T, Keil F,Vahedipour K, et al. MRM 2013, doi: 10.1002/mrm.24901. [4] Heule R, Ganter C, Bieri O. MRM 2013, doi: 10.1002/mrm.24659.
[5] Ma D, Gulani V, Seiberlich N, et al. Nature 2013, 495:187-93. [6] Cheng C-C, Chung H-W, Chao T-C, et al. ISMRM 2013, p. 4216.
[7] Hennig J. Concepts in MR 1991, 3:125:43.
Support from grants R01CA149342, P41EB015898 and R01EB010195 is acknowledged.